

# Doping of Poly(cyclophosphazene–benzoquinone) Films with Polyiodide

Mira Josowicz,\* Jing Li, Charles F. Windisch, Jr., Gregory J. Exarhos, Donald R. Baer, William D. Samuels, and Michelle D. Ulmen†

Pacific Northwest National Laboratory,<sup>§</sup> Richland, Washington 99352

Received February 25, 1997<sup>®</sup>

Polyiodide is inserted into poly(cyclophosphazene–benzoquinone) (PPBQ) film from solution or vapor phase as a result of a charge-transfer interaction between the quinone oxygen and iodine. The incorporation of the polyiodide into the PPBQ film enhanced ion (or electron) transport in the film. Characterization of the PPBQ film before and after polyiodide doping with X-ray photoelectron, UV/vis and Raman spectroscopy indicates that the doping mechanism is governed by the formation of a charge-transfer complex. Raman spectra of PPBQ films suggest that polyiodide interacts with the oxygen atoms in the P–O–C linkage, where the phosphorus atom is part of the phosphazene trimer and the carbon atom is part of the aromatic ring. This is the first direct evidence for the bonding arrangement of iodine in a poly(cyclophosphazene) system.

## Introduction

The electrochemical synthesis of poly(cyclophosphazene–benzoquinone) (PPBQ) material directly at an electrode surface has the potential to provide control of structural, compositional and morphological properties of a three-dimensional network type of coating.<sup>1,2</sup> The cyclomatrix framework is built from repeating open rings formed from cyclophosphazene–benzenoid molecules. The interconnection of the inorganic–organic molecules through a –O– linkage as shown in Figure 1, introduces a large intramolecular barrier for electronic charge transport.

Iodine doping is known to increase the conductivity of many conjugated systems such as polyacetylene,<sup>3</sup> polythiophene,<sup>4</sup> or nonconjugated inorganic polymers such as linear polyphosphazenes.<sup>5</sup> In the few papers published on the interaction of I<sub>2</sub> with polyethers and polyphosphazenes with ether side groups,<sup>5–9</sup> it was proposed that the ether groups assisted disproportionation of I<sub>2</sub> to form polyiodides.<sup>5–7</sup> The argument was based on two important factors. First, the Raman spectra of the I<sub>2</sub>-treated polymers exhibited peaks at

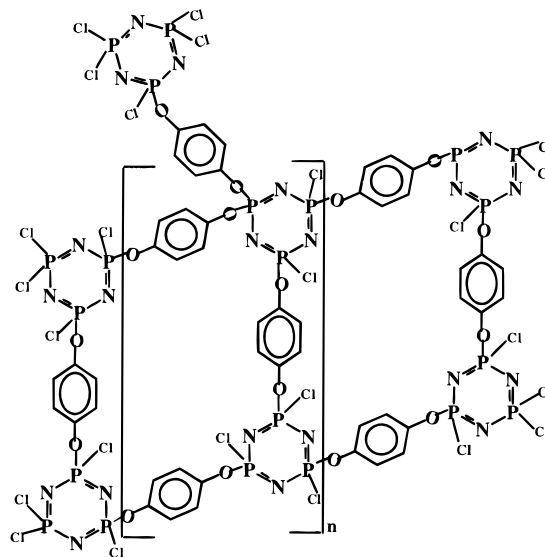


**Figure 1.** Schematic of the electrochemically synthesized PPBQ films.

about 115 and 170 cm<sup>-1</sup> that were assigned to I<sub>3</sub><sup>-</sup> and polyiodide, I<sub>5</sub><sup>-</sup>, respectively. Second, a direct attack of the I<sub>2</sub> on the phosphazene backbone was ruled out because the oxidation potentials were too low. On the basis of these results, an ion-relay mechanism, involving I<sup>-</sup> hopping between polyiodides was proposed to explain the increase in conductivity imparted by I<sub>2</sub> to polyethers and polyether–phosphazene complexes.<sup>5–7</sup> Despite these results, however, direct evidence for how the polyiodide was bound to the polymer was lacking. Bonding in PPBQ is particularly ambiguous since there are at least two sites with significant basicity: the N atom in the phosphazene ring and the O atom in the P–O–C bridge. In addition, aromatic rings are known to interact with halides according to several well-known mechanisms.<sup>10</sup>

(10) Andrews, L. J.; Keefer, R. M. In *Molecular Complexes in Organic Chemistry*; Holden-Day, Inc.: San Francisco, 1964; Chapter 6.

\* To whom correspondence should be addressed.

† AWU-NW Fellow.

<sup>§</sup> Pacific Northwest National Laboratory is a multiprogram national laboratory operated for the U.S. Department of Energy by Battelle Memorial Institute under Contract DE-AC06-76RLO 1830.

<sup>®</sup> Abstract published in *Advance ACS Abstracts*, April 15, 1997.

(1) Josowicz, M.; Li, J.; Exarhos, G. J. *J. Electrochem. Soc.* **1994**, *141*, L162.

(2) Li, J.; Josowicz, M. *Chem. Mater.*, submitted.

(3) Pekker, S.; Janossy, A. In *Handbook of Conducting Polymers*; Skotheim, T. A., Eds.; Dekker: New York, 1986; Vol. 1.

(4) Satoh, M.; Imashi, K.; Yasuda, Y.; Tsumi, R.; Yamasaki, H.; Aoki, S.; Yoshino, K. *Synth. Met.* **1989**, *30*, 33.

(5) Lerner, M. M.; Lyons, L. J.; Tonge, J. S.; Shriver, D. F. *Chem. Mater.* **1989**, *1*, 601.

(6) Lerner, M. M.; Tipton, A. L.; Shriver, D. F. *Chem. Mater.* **1991**, *3*, 1117.

(7) zur Loye, H.; Heyen, B. J.; Marcy, H. O.; DeGroot, D. C.; Kannewurf, C. R.; Shriver, D. F. *Chem. Mater.* **1990**, *2*, 603.

(8) Forsyth, M.; Shriver, D. F.; Ratner, M. A.; DeGroot, D. C.; Kannewurf, C. R. *Chem. Mater.* **1993**, *5*, 1073.

(9) Gleria, M.; Minto, F.; Scoconi, M.; Pradella, F.; Carassiti, V. *Chem. Mater.* **1992**, *4*, 1027.

Raman spectroscopy has the potential to determine which functional sites in PPBQ are bonded to the polyiodide chains. Assuming that several bands in the Raman spectrum of the polymer can be assigned to the vibrational modes of specific functional groups and that the frequency shifts and/or intensity changes of those bands can be discerned, it should be possible to tell how the polyiodide chains are bonded and which bands are affected by the  $I_2$  doping. There are several possibilities why this approach was not taken in the past. First, the Raman bands from polyphosphazene films are very weak and are usually obscured by fluorescence. Most of the previous Raman studies focused on the lower frequency region that contains the relatively strong bands from the iodine species. Second, the polymer films are very easily burned by laser light and require a combination of low laser power, long exposure times, and very sensitive detection to discriminate bands intrinsic to the film from background fluorescence and noise. Finally, the polyphosphazenes are not well characterized by Raman spectra. The sensitivity of detectors for Raman spectroscopy has increased significantly over the past several years, so obtaining spectra on some of these difficult systems (admittedly with relatively low S/N) has now become more feasible.

In this paper, for the first time, iodine doping of a cyclomatrix poly(organophosphazene) polymer was carried out from both the vapor and electrolyte solution phase. The electrochemical doping of the electrically insulating PPBQ was initiated by electrochemical oxidation of iodide. Previous studies showed that, during oxidation, a thick layer of iodine can be observed at the electrode surface when its concentration exceeds the sum of the solubility of iodine in the supporting electrolyte and the concentration of  $I_3^-$  at the surface.<sup>11</sup> The concentration of  $I_3^-$  is governed by the equilibrium constant  $k_{eq} = [I_3^-]/[I_2][I^-]$ , of the reaction  $I_2 + I^- = I_3^-$  (740 L/mol at 25 °C). Consequently, the amount of iodine in the PPBQ material will depend upon the bulk concentration of iodine in the solution and on the rate of formation of the activated complex.

The accommodation of the iodine in PPBQ from the vapor phase is driven by sorption. The sorption depends in a complex way on the interaction energies between the adsorbing iodine species at the interface and on the interaction energies within the bulk of the layer.

A comparison between iodine vapor doping and the electrochemical doping of PPBQ was made by Raman spectroscopy and, based on previous studies of linear polyphosphazenes, used to identify the presence and form of iodine in the PPBQ polymer. In addition, structural information on the interactions of iodine with the PPBQ surface was obtained from X-ray photoelectron spectroscopy (XPS) data. The bulk concentrations of the PPBQ and iodine were characterized with UV/vis spectroscopy. Raman spectra of PPBQ films with and without  $I_2$  were compared by noting which bands were affected by  $I_2$  and which were not. Band assignments, based upon measured Raman spectra of several cyclophosphazene trimers that were also synthesized in our laboratory, were used to interpret the  $I_2$ -induced changes in the spectrum of PPBQ and relate these changes to the structure of the iodine-doped complex (PPBQ- $I_2$ ).

## Experimental Section

PPBQ films were polymerized on the surface of an Au-coated quartz substrate using Ti-W as an adhesion promoting layer. The Au layer was approximately 350 Å thick and the Ti-W layer was approximately 100 Å thick. The polymerization of PPBQ was carried out following published procedures.<sup>1,2,12</sup> In this *in situ* synthesis, a solution containing 0.01 M hexachlorocyclophosphazene,  $[PNCl_2]_3$ , and 0.01 M benzoquinone in acetonitrile,  $CH_3CN$ , with 0.1 M tetrabutylammonium iodide,  $Bu_4NI$ , added as the supporting electrolyte, was electrolyzed to produce quinone radicals in the vicinity of the electrode surface. The quinone radicals undergo a nucleophilic substitution reaction with the chlorine atoms of the hexachlorocyclophosphazene to produce the PPBQ film on the cathode. The films were doped with  $I_2$  in two ways: through electrochemically generated  $I_2$  in a solution of 0.01 M KI in 0.1 M  $H_2SO_4$  and by direct exposure to  $I_2$  vapor.<sup>13</sup>

The resistance of the film was measured using an electrode attachment in a dielectric test fixture device which was connected to a Hewlett-Packard 4142B modular dc source/monitor. The current-voltage curve of the film which was placed between two contact electrodes was recorded in the  $Z$  direction. The voltage applied to the free-standing film was within  $\pm 10$  V for PPBQ and  $\pm 3$  V for the PPBQ-iodine complex, respectively.

XPS measurements were performed with a Perkin-Elmer Physical Electronics Model 560 spectrometer. This model was equipped with a double-pass cylindrical mirror analyzer. A Mg K $\alpha$  anode (1253.6 eV) was employed and operated at 15 keV and 300 W. The survey scans (0–1000 eV binding energy) were recorded with a pass energy of 100 eV. The absolute energy scale and linearity of the analyzer were calibrated to Cu 3p at  $75.14 \pm 0.03$  eV and Cu 2p $_{3/2}$  at  $932.66 \pm 0.03$  eV. On this scale, the hydrocarbon C 1s line typically appears at 284.8 eV.<sup>14</sup> The residual pressure in the spectrometer was approximately  $10^{-8}$  Torr during the data acquisition. The binding energies obtained from the survey spectra are assumed to be good to  $\approx 0.3$  eV. XPS data were obtained from polymer films coated on a Pt foil with and without iodine doping. Binding energies reported are believed to be good to  $\pm 0.015$  eV, based upon instrument performance and spectrum repeatability.

The UV/vis spectra of PPBQ before and after iodine doping were obtained with a Cary 5 UV-vis-NIR spectrophotometer (Varian Inc.) using Cary OS/2 multitasking software. The PPBQ and PPBQ- $I_2$  films were scanned from 200 to 800 nm with a scan rate of 1000 nm/min. A dual beam mode was used with a Au/Ti-W/quartz substrate without film as the reference.

Raman spectra were collected using a Spex Industries Model 1877 triple Raman spectrometer with either the 647.1-nm line of an Omnichrome Model 643-100RS Kr laser or the 488.0-nm line of a Spectra Physics Model 164 Ar ion laser for excitation. The longer-wavelength Kr line was found to give better results for PPBQ films, which tended thermally decompose when interrogated with shorter wavelengths. (Laser power used in all the experiments was kept very low, only a few milliwatts, to avoid burning the sample.) Comparison of spectra obtained at 647.1 and 488.0 nm showed no evidence for resonance enhancement between these wavelengths. A Spex Model 1482 ET Raman microscope was also used in a few cases to interrogate a 2- $\mu$ m-diameter spot, at different optically imaged positions on the film samples; however, most of the spectra were obtained from "macro" measurements, where the laser beam was focused over a much larger area. Comparison of spectra from the "macro" and "micro" experiments and between "micro" measurements at various positions across the films revealed no significant differences.

(12) Li, J. Electrochemically Initiated Polymerization of Hybrid Polycyclophosphazene and Its Application to the Work Function Sensor. Ph.D. Thesis, The University of Utah, 1996.

(13) Li, J.; Janata, J.; Josowicz, M. *Electroanal.* **1996**, *8*, 778.

(14) ASTM Standard E 1523-93 Section 7.2.1.1, *Annual Book of ASTM Standards*, 1996; 3.06, 913.

(11) Bejerano, T.; Gileadi, E. *J. Electroanal. Chem.* **1977**, *82*, 209.

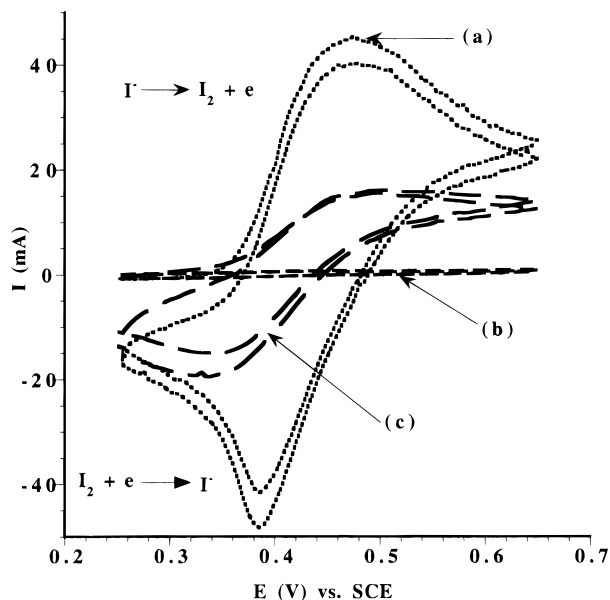


**Figure 2.** Comparison between cyclic voltammograms recorded during oxidation/reduction of iodide in the solution containing 10 mM KI in 0.1 M H<sub>2</sub>SO<sub>4</sub> on (a) bare Pt electrode, (b) on Pt electrode modified with PPBQ film deposited at -1 V = const, and (c) on PPBQ film deposited on Pt electrode at -2 V = const.

All Raman spectra were obtained in the spectrographic mode using a fixed-position grating and a Princeton Instruments LN/CCD detector. The spectral range studied was about 100–1500-cm<sup>-1</sup> Raman shift, which, due to different amounts of dispersion, was acquired with a single grating setting for 488.0-nm excitation but with two grating settings for 647.1-nm excitation. Spectra of samples that did not burn were collected with signal averaging over 10 acquisitions and an exposure time per acquisition of 100 s. Spectra for heat-sensitive samples were averaged from many more acquisitions and over much longer times, up to 3 h in some cases using lower power excitation. The slit width was always 400 μm. For “macro” studies on the films, a 90° scattering configuration was employed with the film sample positioned close to vertical so a scattered line image could be obtained. This arrangement gave the greatest S/N. Spectral analysis was performed using Galactic Industries Grams/368 software (Salem, NH). The estimated uncertainty of the peak frequencies was ±1 cm<sup>-1</sup>.

Raman spectra were obtained for PPBQ films, prepared electrochemically on a Au-coated quartz substrate as discussed earlier.<sup>1,2,12</sup> Raman spectra for neat powders of cyclophosphazene trimers were studied to aid in the assignment of Raman bands, included [NP(O-Ph)<sub>2</sub>]<sub>3</sub> (Ph = phenoxy), [NPCL<sub>2</sub>]<sub>3</sub>, [NP(OCH<sub>2</sub>CF<sub>3</sub>)<sub>2</sub>]<sub>3</sub>, and [NP(N(CH<sub>3</sub>)<sub>2</sub>)<sub>2</sub>]<sub>3</sub>. Spectra of the PPBQ-I<sub>2</sub> films, using doping procedure described above, were acquired with the same parameters as the undoped materials.

## Results and Discussion

**Electrochemistry and Surface Analysis.** Voltammograms for PPBQ-modified Pt electrodes in 1 M H<sub>2</sub>SO<sub>4</sub> plus 10 mM KI solution suggest there is limited surface accessibility in PPBQ-modified electrodes compared to a bare Pt electrode. As shown in Figure 2, currents for the PPBQ-modified electrodes are less than for the bare Pt electrode. The redox peaks for the iodine reactions, however, occur at the same voltages for the PPBQ-modified electrodes and the bare Pt electrode.<sup>15</sup> Direct reaction of PPBQ with I<sub>2</sub> was not likely since the polymer itself is highly resistant to oxidation. Continuous cycling of the PPBQ-modified Pt electrode from 0

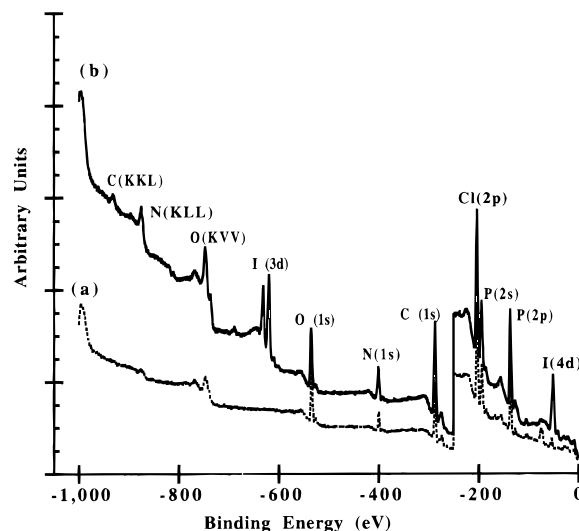


**Figure 3.** XPS surveys of PPBQ films deposited in the presence of Bu<sub>4</sub>NI used as a background electrolyte salt in acetonitrile (a) and of the same film after doping with anodically generated iodine from KI in sulfuric acid (b). (Experimental conditions were the same as given for Figure 2.)

to 0.8 V (SCE) in 1 M H<sub>2</sub>SO<sub>4</sub> plus 10 mM KI solution resulted in an anodic current that steadily rose until a limiting value was obtained signaling the formation of an iodine layer at the electrode surface. Iodine doping in the present study was carried out at a constant potential of 0.8 V (SCE) for 90 min, which was long enough to exceed the solubility limit for I<sub>3</sub><sup>-</sup>. The doping of the PPBQ/Pt substrate from the vapor phase was carried out as described in the literature for the linear polyphosphazene.<sup>7</sup> The substrate was placed above iodine crystals in a sealed bottle at 60 °C for 24 h. After iodine doping, the white PPBQ film became dark brown with a slight metallic luster. The substrates were always equilibrated in air for at least 14 h before further study. From the measured current-voltage curves, the current of the free-standing PPBQ film was found to change linearly with the applied voltage, *U*. From the *I* = *f*(*U*) curve the resistance was calculated to change from the Gohm range (before doping) to 300 KΩ (after doping).

The XPS measurement were made to confirm presence of iodine in the film and to get some information on iodine bonding. The full XPS spectrum of the PPBQ material before and after doping with iodine is shown in Figure 3. The material consists of carbon, nitrogen, phosphorus, chlorine, and oxygen as seen from Figure 1. In addition to the elements of the PPBQ film, after doping with iodine (Figure 3b), intense peaks are observed at 619.8 eV (I) and at 631.4 eV. Both the absolute BEs and the 11.5 eV peak separation are consistent with I 3d<sub>5/2</sub> and I 3d<sub>3/2</sub> peaks, respectively. Using standard *φ* sensitivity factors, the approximate compositions of the iodine doped PPBQ film in relative atomic percent were calculated to be 1.8% for I, 23% for the O, 9% for N, 50% for C, 8% for Cl, and 9% for P. Because of the expected loss of iodine in vacuum, the measured amount of iodine is assumed to be at its lower limit. For the ideal polymer the relative atomic compositions of the primary polymer components O/N/C/Cl/P would be approximately 16/12/49/11/11. The observed values of approximately 23/9/50/8/9 are relatively

consistent with the expected atomic ratios possibly with some extra O (possible due to water in the film) and C (due to handling). Peak ratios for N/P and Cl/P before and after doping with iodine did not change, suggesting the composition of the polymer itself has not been changed.

The difference in the binding energy of the as measured C 1s peak (287.8 eV) and the expected value (284.8 eV) is assumed to be due to specimen charging. Although the C 1s binding energy is known<sup>16</sup> to shift in the presence of oxygen to higher binding energy (by 1.5 eV per C–O bond and to be only slightly affected by X in C–O–X-type bond ( $\pm 0.4$  eV), the ratio of the C–O bonds to C–C and C=C bonds is small and most of the carbon signal is expected to be at 284.8 eV. The observation of specimen charging is consistent with the high resistance of the PPBQ, and it is therefore assumed that all binding energies need to be shifted by approximately 3 eV. The charge corrected binding energy values of the polymer constituents are P 2p 134.7 eV and N 1s 397.4 eV. These values are generally consistent with those previously measured for [NP(OPh)<sub>2</sub>]<sub>3</sub> (P 2p 134.1 eV) and N 1s (398.2 eV), and [NPCl<sub>2</sub>]<sub>3</sub> (P 2p 134.6 eV) and N (1s 398.5 eV).<sup>17</sup>

The small difference in the binding energy between the P 2p bond in the polymer and the phosphazene trimer allows us to make the assumption that chlorine is the most electronegative ligand in the PPBQ structure. The binding energy of the nitrogen in the polymer is the most positive when compared with the other two references. This fact is most likely attributed to an inductive effect of the groups which are not directly bonded to nitrogen.<sup>17</sup> The polarizability of the chloro group in the hexachlorocyclophosphazene was measured to be close to the polarizability of the phenoxy group in the hexaphenoxyposphazene.<sup>17</sup> Using the derived empirical Siegbahn-type relation between the phosphorus binding energy [ $E_b(p)$ ] and effective charge ( $q$ ) on the phosphorus, based on Mulliken population data<sup>17</sup>

$$E_b(p) = 1.67q + 131.6$$

and phosphorus binding energies in PPBQ polymer and reference compounds, the partial charge estimates were made  $q_{PPBQ} = 1.86$ ,  $q_{[NP(O\phi)_2]_3} = 1.49$  and  $q_{[NP(Cl)_2]_3} = 1.79$ . This calculation provides the information that the phosphorus in the PPBQ polymer is in its highest positive charge state and appears consistent with other data to be discussed in this paper. The intense peak of O 1s observed in Figure 3, at the corrected binding energy of 533.1 eV falls within the range of 531–535 eV observed for most polymers.<sup>16</sup> The shifted binding energy for the iodine peaks in PPBQ is 616.8 eV (I 3d<sub>5/2</sub>) and at 628.4 eV of (I 3d<sub>3/2</sub>). The I<sub>2</sub> (3d<sub>5/2</sub>) peak is known to fall around 619.9 eV for I<sub>3</sub><sup>−</sup> (e.g., CsI<sub>3</sub> in the region of 620 eV).<sup>18</sup> The shift of the iodine peak in the PPBQ film to lower binding energies suggests that the iodine species are involved in formation of a charge-transfer complex with electron-donating centers in the film.

**UV/Vis Absorption Spectra.** Changes in the optical absorption spectra of the PPBQ film before and after

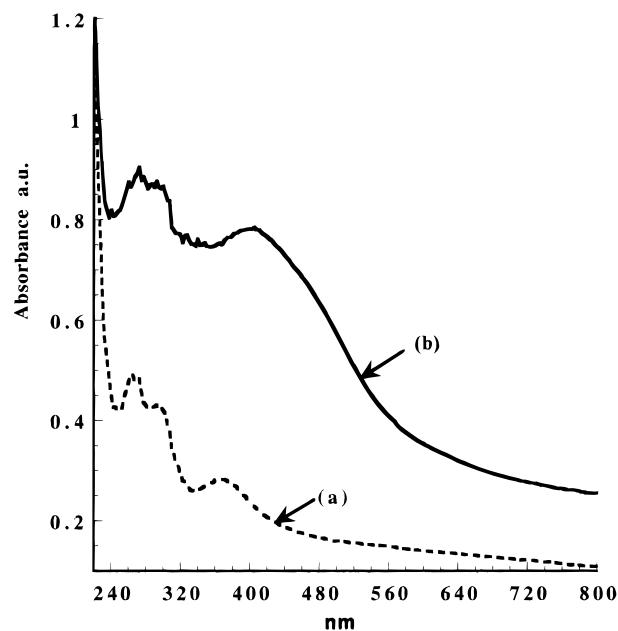


**Figure 4.** UV-vis absorption spectra of PPBQ film as deposited (a) and after doping with iodine (b). Both PPBQ films were obtained the same way as reported in Figure 3.

iodine doping are associated with the formation of a charge-transfer complex (Figure 4). By comparison to spectra of benzoquinone and hydroquinone in acetonitrile solution,<sup>2,12</sup> the peaks at 272 and 298 nm can be assigned to the  $\pi$ – $\pi^*$  transition in their benzenoid forms in the polymer, respectively.

It is known that the effectiveness of quinones as acceptors in electron donor–acceptor (EDA) complex formation depends to some extent on the electron-withdrawing effect of the oxygen atoms. This effect generally leaves the  $\pi$ -system of the quinone electron-deficient and the quinone oxygen correspondingly electron-rich.<sup>19</sup> Consequently, the benzenoid oxygen atoms in the PPBQ film act as good electron donors. This implies that the electron density on the phosphorus is influenced by the mesomeric effects of the phosphazene ring and the Cl substituent. Possibly, the unshared electron pair on the nitrogen and to a smaller extent on the oxygen atom can be conjugated with a 3d orbital of the phosphorus atom and hence reduce its fractional positive charge. The absorbance at 370 nm seen in the spectrum before iodine doping probably arises from the steric and electrostatic effects between the phosphorus of the phosphazene ring and the oxygen of the quinoid structure. The absorption corresponding to the phosphazene P–N=P skeletal bonds is weak and occurs at wavelengths shorter than 200 nm.<sup>20</sup>

The interaction of I<sub>2</sub> with the electron-donor molecules depends on the basicity of the molecules. The interaction of iodine with ethers is weaker than with the stronger bases such as pyridine or thiourea.<sup>5</sup> X-ray diffraction studies established that iodine atoms occur in a one-dimensional chain within a component of the starch, amylase, and give rise to the intense optical absorption around  $\lambda_{max} = 600$  nm.<sup>21,22</sup>

(16) Briggs, D.; Seah, M. P. *Practical Surface Analysis*; Wiley: New York, 1990; Vol. 1.

(17) Dake, L. S.; Baer, D. R.; Ferris, K. F.; Friedrich, D. M. *J. Electron Spectrosc. Relat. Phenom.* **1990**, *51*, 439.

(18) Maki, A. G.; Forneris, R. *Spectrochim. Acta* **1967**, *23A*, 867.

(19) Foster, R.; Foreman, M. I. In *The Chemistry of the Quinoid Compounds*; John Wiley & Sons: London, 1974; Chapter 6, p 257.

(20) Alcock, H. R.; Kugel, R. L. *J. Am. Chem. Soc.* **1965**, *87*, 4216.

(21) Rundle, R.; Baldwin, R. *J. Am. Chem. Soc.* **1943**, *65*, 544.

(22) Teitelbaum, R. C.; Ruby, S. L.; Marks, T. J. *J. Am. Chem. Soc.* **1978**, *100*, 3215.

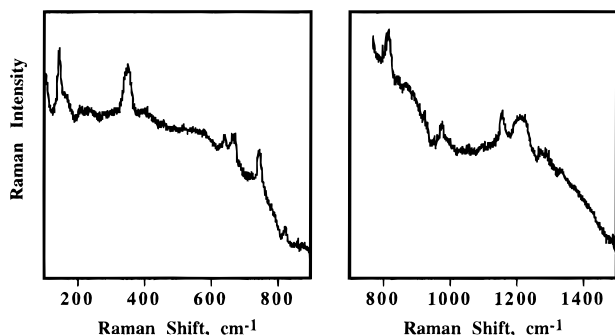


**Figure 5.** Raman spectrum of PPBQ film without background correction.

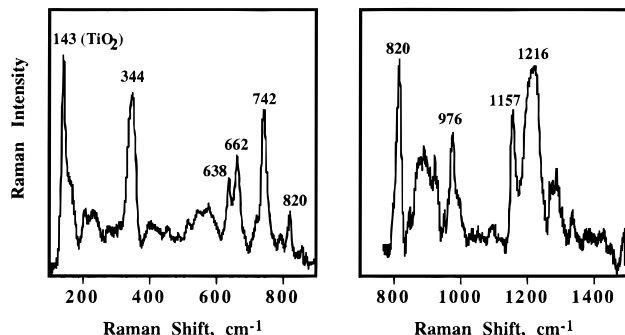


**Figure 6.** Raman spectrum of PPBQ film with background correction.

After the iodine doping of the PPBQ film, the band at 370 nm becomes much stronger and wider and is centered at 403 nm. The red-shift of this band (about 0.27 eV) is a result of donor–acceptor interaction between oxygen and iodine. The direction of the shift reflects the delocalization of electrons within the P–O–C linkage. The increase in the intensity of the absorption indicates an accommodation of iodine in the bulk of the PPBQ. The formation of the charge-transfer complex also affects the  $\pi$ – $\pi^*$  transition. An increase of the absorption intensity ratio of the peak at 298 nm (relative to the peak at 272 nm) represents an additional withdrawal of electrons away from the aromatic ring. Consequently, the strong coupling between the two oscillators, P–O and O–I, contributes to the very high stability of the iodine-doped PPBQ.

**Raman Spectra.** Raman spectra of the PPBQ film, obtained with 647.1-nm excitation, are shown in Figure 5. Significant fluorescence emission was observed along with the weak Raman signals, and this was consistent with fluorometry measurements performed separately. As shown in Figure 6, background subtraction facilitated peak identification; although some broad features, such as the “band” at around 900  $\text{cm}^{-1}$ , are believed to be artifacts resulting from subtracting the strong fluorescence background. Those peaks that are comparatively sharp and clearly stand above the background in Figure 5 are labeled in Figure 6. The peak at 143  $\text{cm}^{-1}$  is believed to arise from anatase ( $\text{TiO}_2$ ) from the substrate. (Ti–W was used as an adhesion promoter for Au sputtering onto the quartz crystal.)

Assigning vibrational modes to the peaks in Figure 6 proved to be difficult because these Raman spectra were the first obtained on this type of poly(cyclophosphazene) film. Attempts to obtain Raman spectra of the  $^{15}\text{N}$ -labeled analogue of the film were unsuccessful. (Since

the synthesis of the labeled film proceeded from very small quantities of labeled starting material, a significantly higher proportion of fluorescence from impurities was observed that completely obscured the Raman signals.) Instead, several cyclophosphazene trimers were synthesized, differing only in the type of side-group substituent. Comparison of Raman spectra of these derivatives with that of the PPBQ helped identify some of the principal peaks in Figure 6 (Table 1). In addition, spectra of the chlorocyclophosphazene trimer (Figure 7) have previously been reported, and normal-coordinate analyses performed.<sup>23</sup>

In making the assignments in Table 1, the Raman spectrum of  $[\text{NP}(\text{Cl})_2]_3$  was used as the principal information source (Figure 7) since this spectrum has been well characterized.<sup>23</sup> Two phosphazene ring modes were assigned in the spectrum of the chloro trimer. The lower frequency mode (667  $\text{cm}^{-1}$ ) was assigned to a ring-breathing mode involving mostly P motion, while the higher frequency mode (784  $\text{cm}^{-1}$ ) was assigned to a ring-breathing mode involving mostly N motion. The spectra of the three other phosphazene trimers in Table 1 also have bands in this region. Since the phosphazene ring exists in all these compounds, although it may be somewhat more distorted in the film and in the trimers with large side groups such as phenoxy, the appearance of these modes in the spectra of all of the compounds studied is not surprising. Consequently, the peaks at 667 and 784  $\text{cm}^{-1}$  in the chloro trimer are believed to correspond to peaks in the 638–662  $\text{cm}^{-1}$  region and at 742  $\text{cm}^{-1}$  in the PPBQ film, respectively, and these are assigned to the two phosphazene ring-breathing modes. The specified lower frequency region in the film (638–662  $\text{cm}^{-1}$ ) actually contains two peaks, at 638 and 662  $\text{cm}^{-1}$ , and it is unclear why two peaks exist instead of one. The reason (which must involve structures unique to the film) may be splitting of the mode due to two types of conformations of the side groups, the different types or degrees of substitution around the phosphazene ring, or the contribution from end groups which generally contain more chloride substituents (Figure 1). However, since the phenoxy trimer has only one peak in this region (Figure 8), it is unlikely that either of the two peaks in the 638–662  $\text{cm}^{-1}$  region of the spectrum of the film arises from functionality other than the phosphazene ring.

The peaks at 820 and 1157  $\text{cm}^{-1}$  in the spectrum of the PPBQ film are believed to arise from stretching modes of the P–O–C linkage. The lower frequency mode involves mostly P–O stretch, while the higher frequency mode is mostly C–O stretch. These assignments are made because the two peaks are missing from spectra of cyclophosphazene trimers with no P–O–C linkage, such as  $[\text{NP}(\text{Cl})_2]_3$  (Figure 7) and  $[\text{NP}(\text{N}(\text{CH}_3)_2)_2]_3$  (Table 1) while they are present in spectra of cyclophosphazene trimers with P–O–C linkage, such as  $[\text{NP}(\text{OPh})_2]_3$  (Figure 8) and  $[\text{NP}(\text{OCH}_2\text{CF}_3)_2]_3$  (Table 1).

The 976  $\text{cm}^{-1}$  peak in the spectrum of the PPBQ film is assigned to the ring-breathing mode of the aromatic ring. The phenoxy trimer has this mode at about 992  $\text{cm}^{-1}$ . It is also the dominating feature in the spectra of most aromatic compounds. It occurs at 991  $\text{cm}^{-1}$  in

(23) Zarian, J. Vibrational Spectroscopic Studies of Poly (dichlorophosphazene) and Relevant Model Compounds. Ph.D. Thesis, The Pennsylvania State University, 1981.

Table 1. Assignments for Key Raman Bands

PPBQ film	[NPCl <sub>2</sub> ] <sub>3</sub>	[NP(O-Ph)] <sub>3</sub>	[Np(OCH <sub>2</sub> CF <sub>3</sub> ) <sub>2</sub> ] <sub>3</sub>	[NP(N(CH <sub>3</sub> ) <sub>2</sub> ) <sub>2</sub> ] <sub>3</sub>	assignment	I effect <sup>a</sup>
638–662	667	616	534–589	524	phosphazene ring mode (mostly P)	Y
742	784	716	727	695	phosphazene ring mode (mostly N)	N
820	815	843			P–O stretch	Y
976 (w)	992				aromatic ring mode	Y
1157	1161	1177			C–O stretch	Y
1216	1252 (w)	1234	1300	1282	P=N stretch	N

<sup>a</sup> N = no effect (or small effect); Y = large effect.

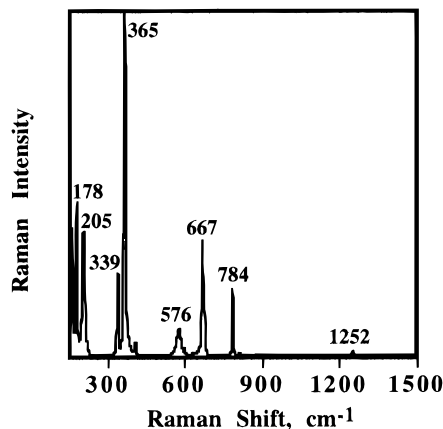


Figure 7. Raman spectrum of chlorocyclophosphazene trimer, [NPCl<sub>2</sub>]<sub>3</sub> powder.

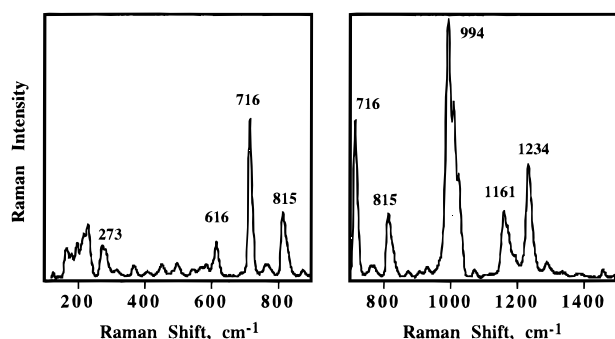


Figure 8. Raman spectrum of phenoxycyclophosphazene trimer, [NP(OPh)<sub>2</sub>]<sub>3</sub> powder.

the spectrum of benzene and at 852 cm<sup>-1</sup> in the spectrum of hydroquinone.

The 1216 cm<sup>-1</sup> peak is assigned to P=N stretch. This assignment was difficult to make because the mode is inactive or very weak in the Raman spectra of some cyclophosphazenes, such as the chloro trimer. The inactivity is believed to be due to the high polarity of the P=N bond, which makes it less polarizable. (The vibration is very strong in the IR spectrum.) Nevertheless, a P=N stretching mode is observed with moderate intensity in several cyclophosphazenes as indicated in Table 1.

The assignment of the strong band in the Raman spectrum of the PPBQ film at 344 cm<sup>-1</sup> is uncertain but may arise from residual unsubstituted PCl<sub>2</sub> bonds (the films were synthesized from the chloro trimer). A very strong band assigned to a PCl<sub>2</sub> bending mode occurs at 365 cm<sup>-1</sup> in the spectrum of the chloro trimer.

Figure 9 shows the effect of iodine doping on the Raman spectrum of the PPBQ film. Doping with electrochemically generated I<sub>2</sub> and I<sub>2</sub> vapor gave the same results except that the electrochemical treatment could be more easily controlled to produce smaller changes in the spectra. For both treatments, the main

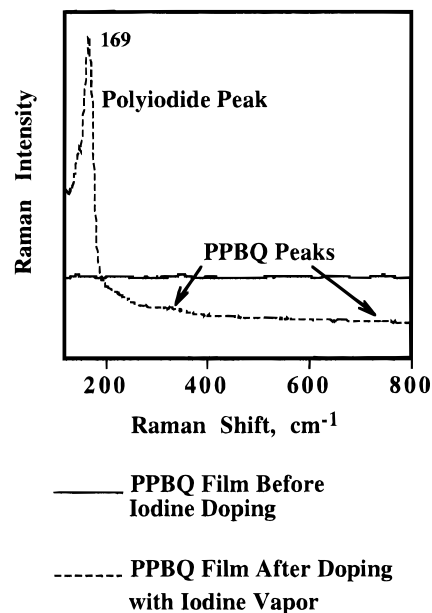


Figure 9. Comparison of Raman spectrum of PPBQ film before and after doping with high concentration of iodine vapor. Figure shows presence of strong polyiodide peak in doped film.

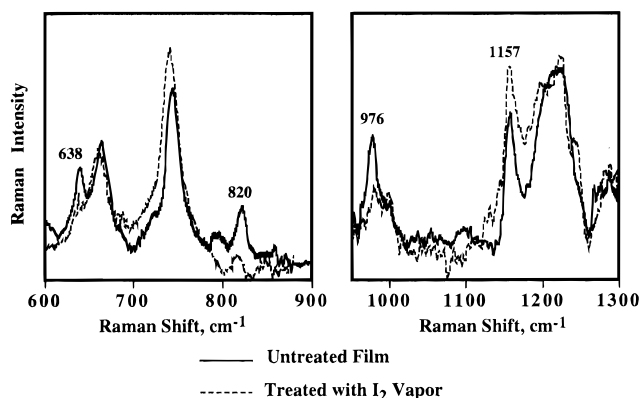


Figure 10. Comparison of Raman spectrum of PPBQ film before and after iodine doping (background corrected) showing effect of iodine on PPBQ vibration modes.

effect of iodine doping on the spectrum was the appearance of a strong band at about 169 cm<sup>-1</sup>. As indicated earlier, this band has been assigned by several authors to polyiodide species.<sup>5-7</sup> The peak was observed in the Raman spectra of several other types of polyphosphazene films. In contrast, the species I<sub>3</sub><sup>-</sup> and I<sub>2</sub> vibrate at about 110 and 216 cm<sup>-1</sup>, respectively.

In addition to the new Raman band assigned to polyiodide, some changes were also observed in the vibrational modes of the PPBQ film. Figure 10 compares the spectrum of the PPBQ film to that of the iodine-treated film (PPBQ-I<sub>2</sub>), after the fluorescence background was removed. Again, some care must be

taken in drawing conclusions because the background subtraction resulted in very "noisy" spectra. A valid comparison of band intensities also relies on referencing the intensities to at least one band that does not change. Unfortunately, no such band occurs for certain in these spectra. However, as shown in Figure 10, qualitative comparison suggests that some of the main bands in the spectrum of the PPBQ film are more affected by the  $I_2$  than others. Table 1 summarizes these results.

In all cases, the primary effect of the iodine appeared to be on the intensities of certain Raman bands and not on the peak frequencies. The reason for this is not certain but may suggest that the bond between the polyiodide and the polymer is too weak to significantly perturb the electron configuration of neighboring bonds but strong enough to influence the symmetry of the normal modes. Another explanation may be that there is a surface enhancement of the withdrawal modes involving certain bonds attached to the metal surface and that these bonds (as well as the degree of enhancement) are influenced by the polyiodide. Selective enhancement is commonly observed in surface-enhanced Raman spectroscopy (SERS).<sup>24</sup> Since the amount of iodine doping in the films was kept small for the Raman studies, the effect of absorption by iodine (Figure 4) on the Raman intensities was not significant. (At higher doping levels, the peak at  $169\text{ cm}^{-1}$  became so large that features in the rest of the spectrum were obscured).

The bands that appeared to be most affected by the presence of iodine are those at  $638\text{ cm}^{-1}$  (decreases relative to the  $662\text{ cm}^{-1}$  band),  $820\text{ cm}^{-1}$  (decreases so that it is almost buried in background noise),  $976\text{ cm}^{-1}$  (decreases), and possibly  $1157\text{ cm}^{-1}$  (increases relative to the  $1216\text{ cm}^{-1}$  band). The band at  $742\text{ cm}^{-1}$  appears to be affected also, but close inspection of the background around this band (especially toward lower frequency) suggests the apparent increase in intensity is probably an artifact of background correction. As shown in Table 1, three of these affected bands have been assigned to P–O–C linkage between the phosphazene ring and the aromatic groups. The  $820$  and  $1157\text{-cm}^{-1}$  bands are proposed to arise directly from P–O and C–O stretching, respectively, while the  $638\text{-cm}^{-1}$  band appears to result from a phosphazene ring mode that involves significant P motion and should, therefore, also be strongly affected by perturbation to the P–O–C bridge. The remaining band that is influenced by  $I_2$ , at  $976\text{ cm}^{-1}$ , is believed to arise from the symmetric ring-breathing mode of the aromatic component.

The results described above suggest that  $I_2$  interacts with the PPBQ films in the form of polyiodide that forms via the disproportionation of  $I_2$  similar to mechanisms proposed for other polymers containing functional groups with sufficient Lewis basicity. Since the  $I_2$  affects primarily those bands associated with the P–O–C linkage, it appears the polyiodide associates with the polymer backbone mainly at the linking O atom. It is not certain why the ring-breathing mode of the aromatic

ring is strongly affected by the  $I_2$  doping (since a direct reaction with the ring does not occur). One possibility is that the symmetry of the aromatic ring vibration is lowered by the polyiodide linkage since the planar conformation of the ring is only stabilized by some 10 kcal over the puckered conformation.<sup>25</sup> In comparison, the symmetry of the phosphazene ring, which is already nonplanar and severely distorted, is probably less perturbed by polyiodide ions attached to the bridging O atom.

## Conclusions

Doping of PPBQ films with either electrochemically generated  $I_2$  or  $I_2$  vapor led to a color change in the film and a decrease in resistance by a factor 4 orders of magnitude. With the XPS measurements the lower limit composition of the PPBQ– $I_2$  surface was determined. Also information about the polarization effects between the Cl–P–O, P–O–C and the  $\text{--N=N--}$  bonds were obtained. Raman spectra of the PPBQ– $I_2$  films indicate the presence of polyiodides, which remain in the film even after standing for several days in an inert atmosphere. Previous studies on other polymer systems suggest that the polyiodides form linear arrays which are in the case of  $I_5^-$  in the form of repeating units ( $\text{I}\cdot\text{I}\cdot\text{I}\cdot\text{I}_2\cdot$ ). They are held inside the PPBQ network. A decrease in the resistance of the PPBQ after iodine doping results from a Grotthus type ion relay mechanism in which the  $\text{I}^-$  ions are shuttled along or between the chains, analogous to the proton conductivity mechanism in aqueous solution.<sup>26–28</sup> The shift of the absorption band from 370 to 403 nm suggests that the bonding with iodine is taking place via the quinone oxygen atoms.

This observation was supported by the Raman spectra that showed the principal influence of  $I_2$  doping was on those bands associated with the P–O–C linkage. The results of this work also strongly suggest that the ability of electron donors containing oxygen to form an electron-donor complex with polyiodide is different from that of electron donors containing nitrogen. An electrostatic interaction, which appears more likely for electron donors containing oxygen, would contribute to relatively small band shifts. The apparent failure of the nitrogen atoms to form an electron donor–acceptor complex with iodine may be due to its higher electron density coupled with a greater tendency to form hydrogen bonds.

**Acknowledgment.** The authors would like to thank Mark H. Engelhard for conducting the XPS experiments. This work has been supported by the DOE's Office of Nonproliferation and National Security Program, and through the office of Basic Energy Sciences, Division of Material Sciences.

CM970119F

(24) Arenas, J. F.; Castro, J. L.; Otero, J. C.; Marcos, J. I. In Proceedings of the XVth International Conference on Raman Spectroscopy. Asher, S. A., Stein, P. B., Eds.; Wiley: New York, 1996; p 684.

(25) Ferris, K. F.; Friedrich, D. M.; Friedman, P. *Int. J. Quantum Chem.* **1988**, 22, 207.

(26) Adams, D. M.; Fernando, W. S. *J. Chem. Soc.* **1973**, 2053.

(27) Manley, T. R.; Williams, D. A. *Spectrochim. Acta* **1967**, 23A, 149.

(28) Emsley, J. *J. Chem. Soc. A* **1970**, 109.